POLITECNICO DI TORINO
Repository ISTITUZIONALE

Durable graphite oxide nanocoating for high performing flame retarded foams

(Article begins on next page)

11 February 2024

Durable graphite oxide nanocoating for high performing flame retarded foams

L. Maddalena, C. Paravidino, A. Fina, F. Carosio [*]

Dipartimento di Scienza Applicata e Tecnologia, Politecnico di Torino, Alessandria campus, Via Teresa Michel 5, Alessandria 15121, Italy

A B S T R A C T

Recent developments in the design of water-based coatings encompassing platelet-like nanoparticles have clearly demonstrated the flame retardant potential of this approach for open cell flexible foams. However, the relatively high number of deposition steps required and the limited reports on the durability of the deposited coatings to multiple compression cycles currently represent the main constraints to this approach. This paper addresses these limitations by exploiting a few steps deposition procedure to produce coatings with durable flame retardant properties. Graphite oxide, sodium alginate and sodium hexametaphosphate were combined in a continuous protective coating that extends to the complex three-dimensional structure of the foam. The flame retardant properties of the coatings were evaluated before and after 1000 compression cycles. Even after such multiple deformations, the coated foams showed no melt dripping and self-extinguishment during flammability tests, as well as a highly reduced heat release rates (-70%) and total smoke release (-70%) during cone calorimetry tests. Furthermore, the ability to withstand the penetration of an impinging flame focused on one side of the coated foam for more than 5 min was also maintained. These results clearly demonstrate the durability of the coated foams, opening to real life application fields such as transports seats where high levels of flame retardancy must be maintained for long time under frequent mechanical stress.

1. Introduction

Open cell polyurethane foams (PU) are widely used in our everyday life as acoustic panel or as main constituent in upholstered furniture. Indeed, through time, PU foams have been employed as padding for seats in transports due to their light weight, affordable cost, easy processability and handling. When employed in seats the function of the PU is to comfortably support the body in static and dynamic conditions by distributing the pression on the cushion and reducing vibrations, ensuring not only a high level of comfort but also safety and protection [1].

The use of PU foams has been favoured through time because they offer a good compromise between market needs and properties that they are able to guarantee over time. Unfortunately, PU are highly flammable and can be easily ignited by a small flame or heat flux quickly leading to a dramatic fire scenario [2,3]. The surface approach to flame retardancy has been recently proposed as a valuable solution capable of efficiently tackle this problem. This approach aims at depositing a functional nanostructured coating on the 3D structure of the foams by direct

impregnation in water-based solution/dispersions of FR chemicals [4]. The most exploited technique to accomplish such coatings is the Layer by Layer assembly (LbL). The LbL is based on the alternate adsorption of oppositely charged polyelectrolytes/nanoparticles by means of a multi-step approach [5–7]. The thickness and properties of the deposited coatings can be modulated by tuning the number of deposition steps, the process parameters and the chemistry of the selected components, making this technique very versatile [8–11]. Moreover, the use of water as solvent and the very low concentrations employed make this technique very attractive as an environmentally friendly process. As far as the use of LbL coatings for PU flame retardancy purposes is concerned, one of the most successful and employed strategy relies on the use of plate-like nano-particles (such as montmorillonite and vermiculite) in combination with a polyelectrolyte matrix. Indeed, the particles high aspect ratios and their inherent thermal stability have been demonstrated to yield coatings capable of shielding heat and reducing volatile release during combustion with strong FR effects [12–14]. Similarly, LbL structures comprising a positively charged polyelectrolytes and high aspect ratio graphene oxide platelets have been also assembled as flame

retardant coating on open cell PU foams. It has been demonstrated that a 3 bi-layer (BL) assembly can easily prevent the collapsing of the foam structure during combustion thus suppressing the melt dripping typical of PU foams while also considerably reducing the rate of combustion [15]. A 6 BL coating has been found capable of limiting the ignitability of the foams when tested by cone calorimetry. The inclusion of a phosphate salt within the coating allowed for a further improvement in the FR properties by reducing to 3 the number of BL needed to observe a non-ignitability behaviour [16]. The effects of plate-like particles of different dimensions has been recently investigated highlighting how the FR performances of the coatings are strongly dependant on their lateral size [17,18]. Indeed, high aspect ratio nanoplates can overlap more efficiently with respect to low aspect ratio ones and thus can produce a more effective barrier to volatiles and heat [18–21]. Although the use of high aspect ratio nanoparticles is capable of considerably improving the efficiency of the achieved FR coatings, these coatings still suffer from limited up-scalability due to the mandatory multi-step nature of the process. In order to address this latter constraint, few-steps and single-step deposition procedures have recently attracted great interest [22,23]. These approaches try to mimic the layered structure that is normally achieved in LbL assemblies by depositing the functional coating constituents with a limited number of steps. For example, nacre-like structures comprising platelet-like particles and a polyelectrolyte binder have been deposited on PU foams achieving FR results comparable to LbL coatings [24,25]. Nevertheless, beside some preliminary studies [12], there is limited knowledge on the actual durability of such surface FR solutions in relation to real application of PU foams as cushioning solutions in transportation or upholstered furniture. Such applications would indeed require the foam and its surface treatment to withstand numerous compression cycles while maintaining a good level of fire protection [17].

To address these limitations, in this work we evaluate the durability of the FR performances conferred to PU foams by a water-based FR coating obtained by a few-step deposition approach, recently developed by our research group [26]. Graphite oxide nanoplates (GO), sodium alginate (SA) and sodium hexametaphosphate salt (SHMP) are selected as constituents for the functional FR coating (Fig. 1).

In the coating composition high aspect ratio GO acts as bricks, which favourable in plane orientation helps in producing a functional barrier during combustion [27]. SA, a water-soluble natural polysaccharide extracted from brown algae, is employed as the continuous matrix [28]. SHMP is employed as char promoter for SA [29,30]. The coating morphology has been evaluated by SEM. Reaction to fire and resistance to fire properties have been evaluated by flammability, cone calorimetry

and flame penetration tests. These characterizations have been performed on the coated foams before and after 200 and 1000 compression cycles in order to evaluate the durability of the flame retardant properties to multiple deformations.

2. Materials and method

2.1. Materials

PU foams with density 20 kg/m^3 and thickness of 60 mm were purchased from a local warehouse. 1 wt% graphite oxide (GO) suspensions were purchased by Avanzare Innovacion Tecnologica S.L (Navarrete, La Rioja, Spain), polyacrylic acid (PAA, solution average Mw ~100,000, 35 wt.-% in H$_2$O), polydiallylammonium chloride (PDAC, average Mw 400,000–500,000, 20 wt% in H$_2$O), sodium hexametaphosphate (SHMP) and sodium alginate (SA, powder) were purchased from Sigma-Aldrich S.r.l. (Milano, Italy). Solutions and suspensions employed in this work were prepared using ultrapure water having a resistance of 18.2 MΩ, supplied by a Q20 Millipore system (Milano, Italy). A 2wt% suspension of GO/SA/SHMP was prepared with a weight ratio of 1wt% GO:0.1%wt SA:1wt%SHMP of solid.

2.2. Coating deposition

Prior the deposition, PU foams were washed with ultrapure water and dried at 80 °C in a ventilated oven. The PU surface was activated by the deposition of a PAA/PDAC bi-layer in order to enable the deposition of the selected GO/SA/SHMP components that bear negative charges. PAA was used as first anchoring layer due to its ability to form hydrogen bonds with PU urethanes functional groups.

Then, PDAC is deposited on PAA by electrostatic interactions yielding a strong positive electrostatic charge and thus preparing the surface for the subsequent adsorption of GO/SA/SHMP. In details, the PU foams were dipped in the 1 wt% PAA solution for 10 min. During this step, the foams were squeezed several times to completely fill the foam volume with the solution. The foams were washed by squeezing in water to remove the excess polyelectrolyte. The same procedure was then employed for the subsequent PDAC layer, which produces a positively charged surface. After the deposition of the PAA/PDAC bilayer, the wet foams were transferred into aluminium molds fitting the foam dimensions (either $100 \times 100 \times 60$ mm^3 or $150 \times 50 \times 60$ mm^3). The GO/SA/SHMP suspension was poured on the top of the foam (150 ml of suspension for every $50 \times 50 \times 60$ mm^3 of sample) completely filling the volume available. During this step the GO/SA/SHMP suspension can
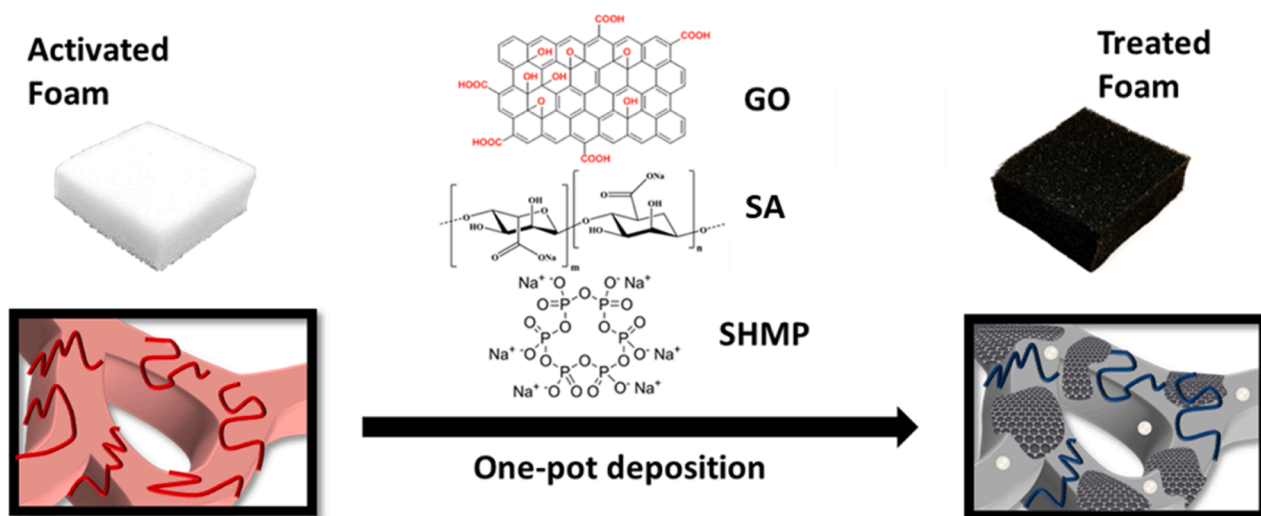

Fig. 1. Schematic representation of the deposition procedure adopted in this work.

easily impregnate the PU structure thanks to the pre-existing PAA/PDAC wet layer. Once fully impregnated the foams were also gently squeezed in order to remove trapped air. The so-treated foams were then dried to constant weight in a ventilated oven at 80 °C for at least 48 h. The final add-on was found to be 113 ± 8% with a density of 44±1 kg/m^3. In the following, treated PU are labelled as PU GO. A number is added (PU GOn) to point out whether the sample has been subjected to compression cycles: for example, PU GO200 indicates that the coated foam has been subjected to 200 compression cycles.

2.3. Characterization

The surface morphology was investigated by Field Emission Scanning Electron Microscopy (FESEM, Zeiss Merlin 4248, beam voltage: 5 kV). Samples were cut, pinned up on conductive adhesive tapes and chromium coated prior to FESEM observations. Mechanical properties were investigated in compression mode on $100 \times 100 \times 60$ mm^3 sample using an INSTRON 5956 equipped with a Foam fixture 10 kN (ASTM 3574) plate following the DIN EN ISO 2439 normative (the fourth compression cycle is considered as representative of the foam initial mechanical properties). The durability of the coating was assessed by performing sets of 200 compression cycles (60% compressive strain, 100 mm/min compression rate) up to a total of 1000, on foam slabs with dimensions of either $100 \times 100 \times 60$ mm^3 or $150 \times 50 \times 60$ mm^3. After 200 and 1000 compression cycles, the slabs were cut to obtain the required number of specimens having dimensions needed for each functional characterization. Flammability tests were performed in horizontal configuration following the UL 94 –HF ASTM D 4986 standard, equivalent to ISO 9772 standard, by applying a 70 mm methane flame for 60 s on the short side of samples ($50 \times 150 \times 13$ mm^3). The test was repeated 4 times for each of the PU GOn and results averaged. During the tests, parameters such as self-extinguishment, final residue and formation of incandescent droplets of molten polymer were evaluated. Cone calorimetry (Noselab ATS, Nova Milanese (MB), Italy) was employed in order to investigate the combustion behaviour. Square planar samples ($100 \times 100 \times 20$ mm^3) were analysed under 25 kW/m^2 irradiative heat flux according to the ISO 5660 standard. Measurements were performed in quadruplicate for each PU GOn evaluating Time to Ignition (TTI), Peak of Heat Release Rate (pkHRR), average Heat Release Rate (avHRR), Total Heat Release (THR), Total Smoke Release (TSR), Smoke Production Rate (SPR) and final residues. Flame penetration tests were performed to assess the resistance of coated samples to the penetration of a small flame generated from a butane flame torch (estimated power at maximum flow rate with premixed flame, 150 W). The test was carried out by placing square specimens ($50 \times 50 \times 20$ mm^3) in a ceramic frame, held in vertical position. The torch, positioned at 100 mm distance from the surface of the specimen, was applied continuously toward the specimen centre for 5 min. The temperature profiles on the front side surface (exposed to the flame) and on the back side of the specimen were measured by two thermocouples (stainless steel sheathed K-type; 1 mm diameter). The thermocouples were placed into contact with the specimen and fixed ensuring that no change in positioning occurs during the test. The test was duplicated for each different PU GOn. Post combustion residues were imaged by SEM (EVO 15, Zeiss, Germany, beam voltage 20 kV). Samples were mounted on a conductive tape in cross section and gold sputtered before measurements.

3. Results and discussion

3.1. Coating morphology

The change in surface morphology after the deposition of the coating was investigated by SEM (Fig. 2).

Neat PU shows the typical 3D structure of open cell foams where the cellular skeleton consists of struts and joints produced during the foaming process. High magnification micrographs point out a rather smooth surface with wrinkled edges. The deposition of the GO-based coating produces a continuous coating capable of conformally adapt to the native open 3D structure of the foam without occluding the open pores. This is achieved thanks to the favourable aspect ratio of the adopted GO that allows the nanoplates to bend around the edges and produces a thin compact coating where multiple plates overlap on top of each other maximizing surface coverage.

3.2. Mechanical behaviour and morphological investigation

The mechanical properties of the obtained samples were assessed by compression test. In addition, the coated foams were also subjected to 1000 compression cycles in order to investigate the effects of a continuous cyclic deformation on the coating morphology and functional FR properties. Fig. 3 reports the collected stress/strain plots and FE-SEM images of the coated foam after 4, 200 and 1000 compression cycles.

The untreated PU shows the typical 3 phase compressive/stress curve of an open cell foam (Fig. S1) [1]. [31], Below 10% compression the foam acts similarly to a linear elastic material corresponding to the reversible deformation of PU foam walls. Between 15 and 40% of compression the walls of the cellular structure undergo progressive buckling, eventually reaching a densification stage where the cell walls crush together and the compressive stress steeply increases. Upon unloading, the foam recovers its deformation producing a typical hysteresis plot. This ability is partially maintained after 200 compression cycles as the initial portion of the loading curve is shifted to the right indicating a partial recovery of the deformation (Fig. S2). This, can be related to the employed deformation rate and the limited resting time between each loading/unloading cycle.

The presence of the coating considerably changes the mechanical response of the foam, showing higher stress values, in the whole range of deformation, compared to the unmodified PU. 100 kPa are required to
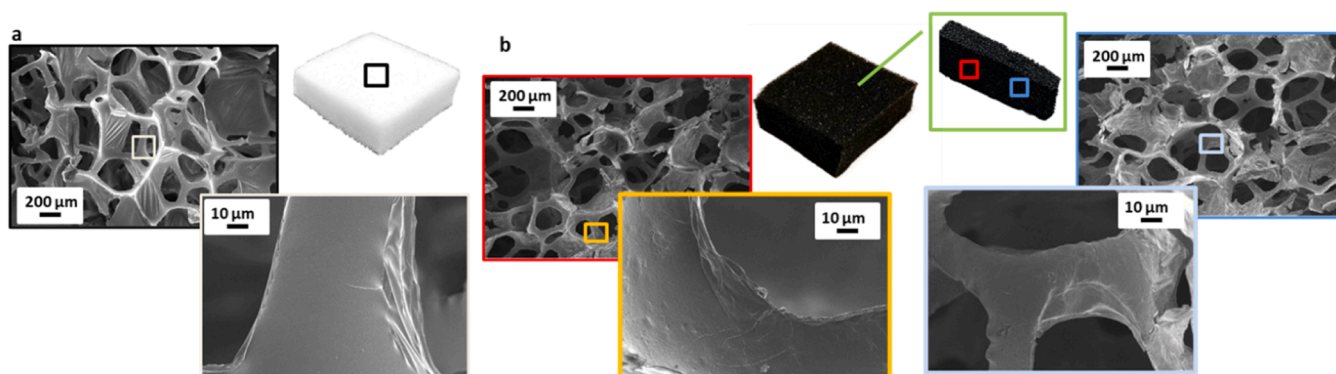

Fig. 2. Morphologies of PU foam before (a) and after (b) deposition (PU GO).
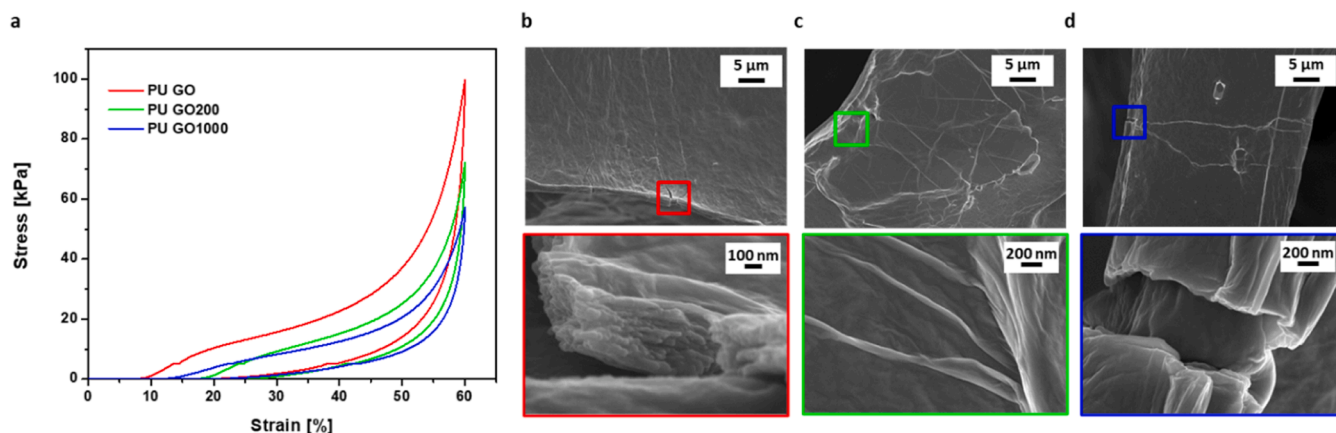
Fig. 3. Compression cycles performed on PU GO; cycles 4, 200 and 1000 (a), FE-SEM imagine of PU GO subjected to 4 (b), 200 (c) and 1000 (d) compression cycles.

achieve a 60% compression on PU GO while only 6 kPa are needed to obtain the same deformation on PU. In addition to the obvious twofold increase in density, such strong increase in stress can be ascribed to the presence of GO nanoplates and the inherent stiffness of the coating that stems from the ionic interactions occurring at molecular scale [32]. This is in agreement with previous works where similar increases in stiffness were observed for PU foams coated by LbL assemblies encompassing nanoparticles [17,26]. Interestingly, the stress/strain plot still show an hysteresis loop thus suggesting that the ability to recover the deformation is not prevented by the presence of the coating. When subjected to multiple compression cycles the coated foam hysteresis loop shows a partial recovery of the deformation as already observed for the neat PU (Fig. S2). The stiffness of the coated foam, evaluated as the stress at 40% strain, is reduced by 33% after 200 cycles and by 45% after 1000 cycles indicating that a minor reduction occurs over 800 compression cycles. This suggests that the coated foam would display a firm behaviour through the 1000 compression cycles thus falling within the range of denser flexible PU foams (e.g. 50–70 kg/m^3). FESEM observations performed on coated samples compressed at different cycles allow for an evaluation of the coating structural integrity upon cyclic compression. Upon multiple deformation, cracks of different size are formed as the coating needs to comply with the collapsing structure of the PU foam (Fig. 3b, c and d). Interestingly, the formation of such cracks does not compromise the coating adhesion to foam as clearly visible in low magnification micrographs, where the continuity of the coating is clearly preserved (Fig. S2), evidencing no significant coating delamination. This can be ascribed to the deposited activation bilayer that promotes optimal bonding between the PU surface (by hydrogen bonds) and the deposited functional coating (by electrostatic interactions). Based on the FESEM evidences it is possible to hypothesize a mechanism where the cracks gradually growth during the first compression cycles eventually reaching a plateau after which no substantial increase occurs.

3.3. Flame retardant characterization

The coated foam reaction to the exposure to a flame and heat flux was evaluated by flammability test and cone calorimetry, respectively.
Table 1 reports data from flammability tests performed on neat PU,

PU GO, PU GO200 and PU GO1000. Fig. S3 collects pictures of obtained residue from PU GO, and PU GO1000.

During the test the neat PU ignites during the 60 s flame application with the flame quickly spreading to the entire length of the sample. Incandescent melt droplets (igniting the dry cotton placed underneath the sample) are constantly produced as the advancing flame completely consumes the foam leaving no residue (Fig. S3). The deposition of GO/SA/SHMP coating drastically changes the flammability behaviour of the PU foams that can easily withstand the 60 s flame application showing no flame spread. Once the methane flame is removed the coated samples show either a self-extinguish behaviour where a small flame remains confined for 23–26 s within 2 cm from the specimen edge before extinguishing or a non-igniting behaviour with the total absence of flame. The melt-dripping phenomenon is completely suppressed. Surprisingly, samples subjected to 200 and 1000 compressing cycles maintained the same performance of the uncompressed ones, within the experimental deviations of after flame time and residual mass. Cone calorimetry tests were performed to evaluate behaviour of untreated and treated foams when exposed to a heat flux commonly found in the early stage of a fire (25 kW/m^2) [33]. Fig. 4 collects HRR, THR, SPR and TSR plots vs. time as well as histogram of the main parameters evaluated during the test (numerical values are collected in Table S1).

During the test, the neat PU foam quickly ignite and its 3D structure collapses forming a low viscosity liquid and reaching the maximum HRR value. This behaviour is normally deemed dangerous as it has been correlated with an increase fire spread in real scenarios [2]. In strong contrast with the neat PU the coated foam shows a totally different burning behaviour. Indeed, the collapsing is prevented and HRR values remain extremely low, yielding a pkHRR of only 84 kW/m^2 (i.e. a 71% reduction with respect to the uncoated foam). Smoke parameters are also reduced as demonstrated by a conspicuous reduction in TSR (−70%). The residue collected at the end of the test displays the same structure and shape of the starting foam and accounts for 52% of its mass (Fig. S4). Compressed foams yielded pkHRR and TSR results similar to the uncompressed ones thus further demonstrating the durability of the deposited coating. THR values show a slight increase likely ascribed to the formation of cracks within the coating as reported in Fig. 3. Post combustion residue collected after cone calorimetry tests were analysed

Table 1
Comparison between flammability behaviour of neat PU and PU GO, PU GO200 and PU GO1000 treated samples.

Sample	Melt-dripping	Self-extinguishment	After flame time[*]	Damaged length	Residue ± σ [%]
PU	Yes	No	–	–	No
PU GO	No	Yes (2 out of 4 showed no ignition)	25 ± 2	<2 cm	95 ± 2
PU GO200	No	Yes (3 out of 4 showed no ignition)	23 ± 1	<2 cm	96 ± 2
PU GO1000	No	Yes (2 out of 4 showed no ignition)	26 ± 5	<2 cm	93 ± 4

[*] The time the flame persists after the removal of the ignition source.
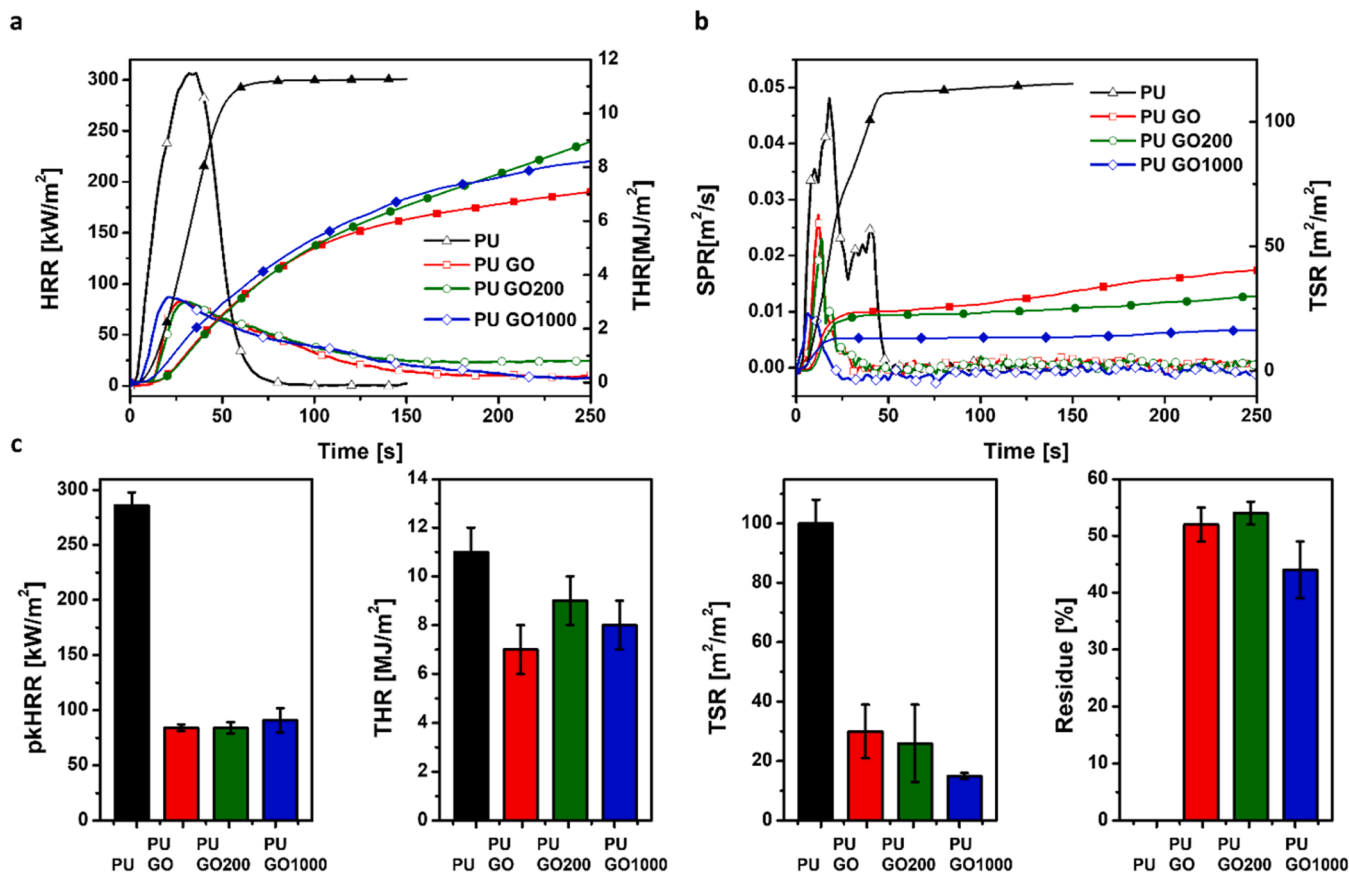
a

b

c

Fig. 4. Cone Calorimetry test results of PU, PU GO, PU GO200, PU GO1000: (a) Heat release rate (HRR, empty symbol+solid line) vs time and total heat release vs time (THR, symbol+solid line), (b) smoke production rate (SPR, empty symbol+solid line) vs time and total smoke release vs time plots (TSR, symbol+solid line), (c) residues, peak of heat release rate (pkHRR), total heat release rate (THR) and total smoke release comparison of tested samples (TSR).

by SEM. Collected micrographs are reported in Fig. 5.

Low magnification micrographs clearly show the original 3D structure of the as-prepared foams is preserved. It is worth noticing that, although the open cell structure is maintained after combustion, the resulting structure is extremely brittle, as testified by the presence of numerous debris and cracks. This is related to the formation of a hollow charred exoskeleton due to the almost complete pyrolysis of the PU during combustion. Such structure is mostly comprised by GO nanoplates held together by a carbonaceous char promoted by SHMP and is responsible for the observed impressive fire retardant properties displayed by the treated PU foams. Indeed, the presence of such charred exoskeleton can exert a FR effect on different levels. On a macroscopic scale, it efficiently prevents foam collapsing during combustion with a direct effect on melt-dripping during flammability and the formation of the pool of polyols and the related steeply increase in HRR during cone calorimetry [34]. On a microscopic scale, the presence of highly orientated GO nanoplates embedded within a charred residue can efficiently hinder the release of PU decomposition products through a tortuous path mechanism and/or absorption [35]. This limits the rate of volatiles feeding the flame which consequently leads to a quick self-extinguishing mechanism as well as reduced heat release and smoke production rates as observed during flammability and cone calorimetry tests, respectively.

3.4. Flame penetration tests

In addition to the characterization of reaction to fire, resistance to fire was also assessed by means of flame penetration tests. During the test, the sample is placed in a ceramic frame and one side is exposed to a butane flame positioned at a fixed distance. Two thermocouples are

employed to monitor the temperature on the exposed and unexposed sides of the samples. The occurrence of flame penetration and the time at which it occurs are monitored during the test. Fig. 6 reports the images of the uncoated and coated foams during the test and the temperature plots for each tested sample, whereas Fig. S5 shows pictures of samples cross-sections collected after the test.

PU foams are not designed for resistance to fire test as testified by the nearly instantaneous failure of the untreated sample. Indeed, upon exposure to the flame torch the flame is immediately capable of piercing through the sample that is completely destroyed (Fig. 6a). Conversely, treated foams can withstand the penetration of the flame for the whole duration of the test as demonstrated by a stable temperature plateau established on the unexposed side of the foam after a reaching a maximum value recorded around 150 s. This latter phenomenon can be ascribed to foam/coating charring and oxidation processes occurring within the foam during the first minutes of flame application [36]. The temperature at the unexposed side of the samples is maintained below 160 °C for all tested samples with slight improvements for PU GO200 and PU GO1000. As observed for flammability and cone calorimetry tests PU GO200 and PU GO1000 maintain performances similar to PU GO thus highlighting how the extraordinary FR properties of this GO-based coating are durable to multiple compression cycles.

4. Conclusions

In this paper, graphite oxide-based coatings have been deposited on flexible open cell PU foams. The achieved flame retardant performances and their durability to multiple compression cycles has been thoroughly investigated. The deposition procedure yields a homogeneous coating on the complex 3D structure of the foam capable of increasing the foam
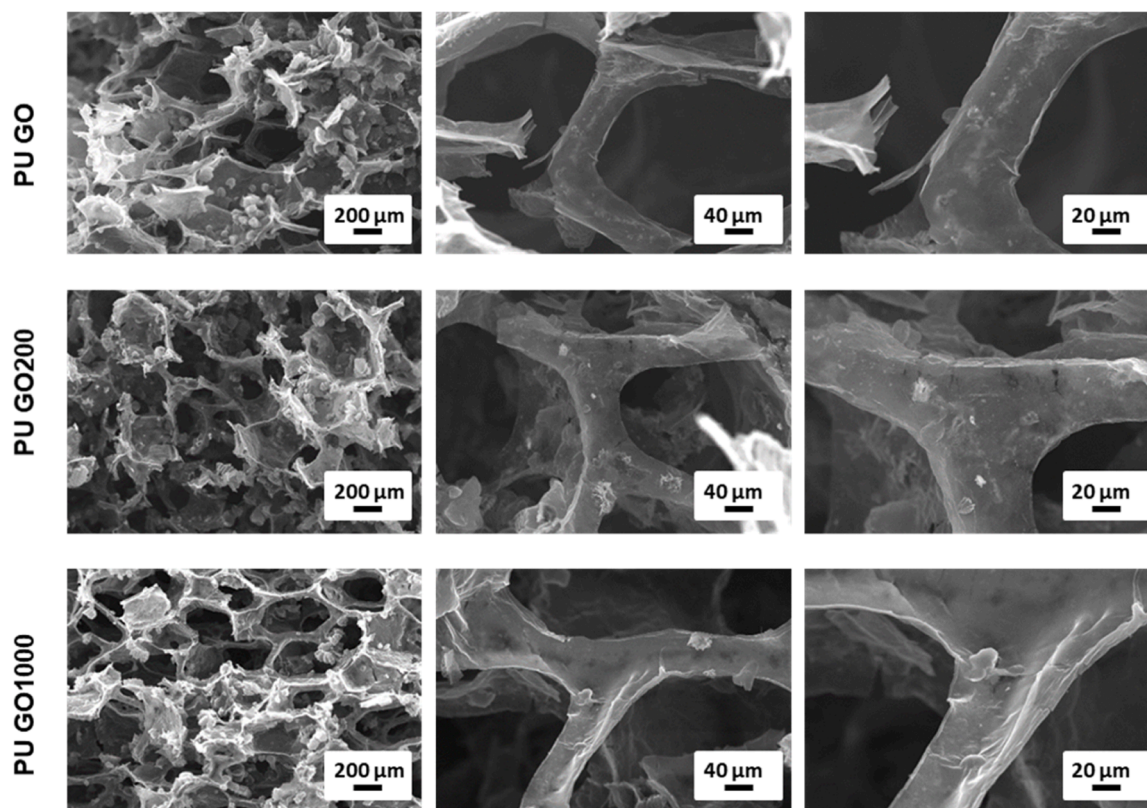
Fig. 5. SEM imaging of post combustion residue from cone calorimetry measurements.
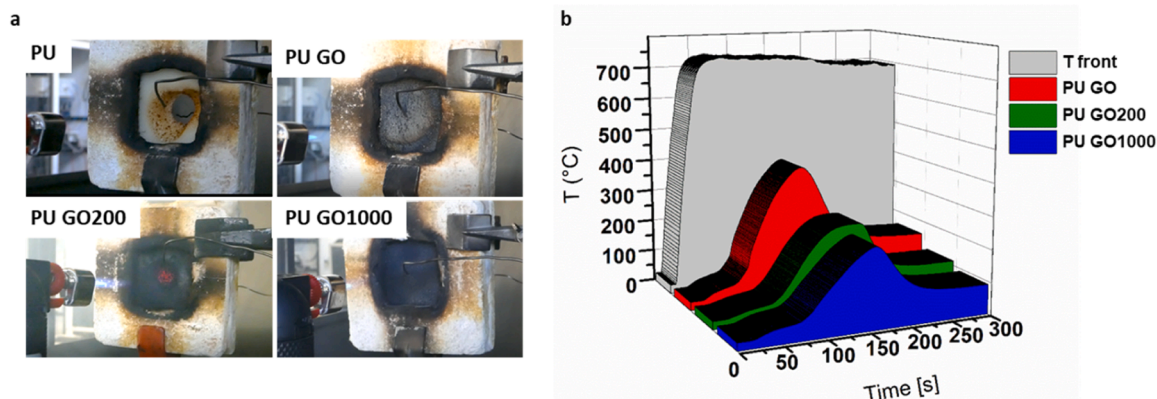

Fig. 6. Flame penetration test screenshot of uncoated (5 s) and coated foams (300 s) during the test (b)temperature plots for all testes samples (b).

compressive strength while maintaining the ability of recovering the deformation typical of flexible foams even after 1000 compression cycles. The flame retardant characterization points out how the presence of the coating can easily suppress melt dripping and grant a self-extinguishing behaviour during flammability tests as well as considerably reduce the heat release rate (−70% in pkHRR) and the total smoke release (−70% in TSR) during cone calorimetry test. During flame penetration tests the coated foams managed to withstand the penetration of an impinging flame (T on exposed surface $\approx 700\,°C$) while successfully shielding the opposite side for more than 5 min even. Such impressive flame retardant properties were totally maintained after 1000 compression cycles, clearly demonstrating that the coating ability to deliver flame retardant effects is not compromised upon repeated deformations. The achieved results clearly support the potential use of these GO-based coatings as industrially viable, highly effective and

durable flame retardant solution for practical applications where multiple deformation cycles are foreseen during the foam lifespan.

Compression tests of neat PU, low magnification micrographs of as prepared and compressed PU GO, snapshots of neat PU during flammability test and images of PU GO and PU GO1000 after the tests with marked damaged zone, images of cone calorimetry test residues, cone calorimetry test results and images of the residues collected after flame penetration are supplied as Supplementary material.

CRediT authorship contribution statement

L. Maddalena: Conceptualization, Methodology, Validation, Investigation, Data curation, Writing – original draft. **C. Paravidino:** Investigation, Validation, Data curation. **A. Fina:** Writing – review & editing. **F. Carosio:** Conceptualization, Writing – review & editing, Supervision,

Funding acquisition.

Declaration of Competing Interest

The authors declare that they have no known competing financial interests or personal relationships that could have appeared to influence the work reported in this paper.

Data availability

Data will be made available on request.

Acknowledgments

Supplementary materials

Supplementary material associated with this article can be found, in the online version, at doi:10.1016/j.polymdegradstab.2023.110422.

References

[1] W.N. Patten, S. Sha, C Mo, A vibrational model of open celled polyurethane foam automotive seat cushions, J. Sound Vib. 217 (1) (1998) 145–161.

[2] R.H. Krämer, M. Zammarano, G.T. Linteris, U.W. Gedde, J.W. Gilman, Heat release and structural collapse of flexible polyurethane foam, Polym. Degrad. Stab. 95 (6) (2010) 1115–1122.

[3] A.B. Morgan, Revisiting flexible polyurethane foam flammability in furniture and bedding in the United States, Fire Mater. 45 (1) (2021) 68–80.

[4] G. Malucelli, F. Carosio, J. Alongi, A. Fina, A. Frache, G. Camino, Materials engineering for surface-confined flame retardancy, Mater. Sci. Eng. R Rep. 84 (2014) 1–20.

[5] G. Decher, J.D. Hong, J. Schmitt, Buildup of ultrathin multilayer films by a self-assembly process: III. Consecutively alternating adsorption of anionic and cationic polyelectrolytes on charged surfaces, Thin Solid Films 210-211 (1992) 831–835.

[6] G. Decher, Fuzzy Nanoassemblies: toward Layered Polymeric Multicomposites, Science 277 (5330) (1997) 1232–1237.

[7] R.K. Iler, Multilayers of colloidal particles, J. Colloid Interface Sci. 21 (6) (1966) 569–594.

[8] Park SY, M.F. Rubner, A.M. Mayes, Free energy model for layer-by-layer processing of polyelectrolyte multilayer films, Langmuir 18 (24) (2002) 9600–9604.

[9] R.L. Abbett, Y. Chen, J.B. Schlenoff, Self-exchange of polyelectrolyte in multilayers: diffusion as a function of salt concentration and temperature, Macromolecules 54 (20) (2021) 9522–9531.

[10] N.K. Mishra, N. Patil, S. Yi, D. Hopkinson, J.C. Grunlan, B.A. Wilhite, Highly selective hollow fiber membranes for carbon capture via in-situ layer-by-layer surface functionalization, J. Memb. Sci. 633 (2021), 119381.

[11] M. Lundin, F. Solaqa, E. Thormann, L. Macakova, E. Blomberg, Layer-by-layer assemblies of chitosan and heparin: effect of solution ionic strength and pH, Langmuir 27 (12) (2011) 7537–7548.

[12] F. Carosio, A. Fina, Three organic/inorganic nanolayers on flexible foam allow retaining superior flame retardancy performance upon mechanical compression cycles, Front. Mater. 6 (20) (2019).

[13] P. Chen, Y. Zhao, W. Wang, T. Zhang, S Song, Correlation of montmorillonite sheet thickness and flame retardant behavior of a chitosan–montmorillonite nanosheet membrane assembled on flexible polyurethane foam, Polymers (Basel) 11 (2) (2019) 213.

[14] S. Qin, M.G. Pour, S. Lazar, O. Köklükaya, J. Gerringer, Y. Song, et al., Super Gas Barrier and Fire Resistance of Nanoplatelet/Nanofibril Multilayer Thin Films, Adv Mater Interfaces 6 (2) (2019), 1801424.

[15] L. Maddalena, F. Carosio, J. Gomez, G. Saracco, A. Fina, Layer-by-layer assembly of efficient flame retardant coatings based on high aspect ratio graphene oxide and chitosan capable of preventing ignition of PU foam, Polym. Degrad. Stab. 152 (2018) 1–9.

[16] F. Carosio, L. Maddalena, J. Gomez, G. Saracco, A. Fina, Graphene oxide exoskeleton to produce self-extinguishing, nonignitable, and flame resistant flexible foams: a mechanically tough alternative to inorganic aerogels, Adv. Mater. Interfaces 5 (23) (2018), 1801288.

[17] L. Maddalena, J. Gomez, A. Fina, F Carosio, Effects of graphite oxide nanoparticle size on the functional properties of layer-by-layer coated flexible foams, Nanomaterials 11 (2) (2021) 266.

[18] A.A. Cain, M.G.B. Plummer, S.E. Murray, L. Bolling, O. Regev, J.C. Grunlan, Iron-containing, high aspect ratio clay as nanoarmor that imparts substantial thermal/flame protection to polyurethane with a single electrostatically-deposited bilayer, J. Mater. Chem. A 2 (41) (2014) 17609–17617.

[19] H. Yang, B. Yu, P. Song, C. Maluk, H. Wang, Surface-coating engineering for flame retardant flexible polyurethane foams: a critical review, Compos. Part B Eng. 176 (2019), 107185.

[20] G. Laufer, C. Kirkland, A.A. Cain, J.C Grunlan, Clay–chitosan nanobrick walls: completely renewable gas barrier and flame-retardant nanocoatings, ACS Appl. Mater. Interfaces 4 (3) (2012) 1643–1649.

[21] S. Lazar, F. Carosio, A.-L. Davesne, M. Jimenez, S. Bourbigot, J. Grunlan, Extreme heat shielding of clay/chitosan nanobrick wall on flexible foam, ACS Appl. Mater. Interfaces 10 (37) (2018) 31686–31696.

[22] E.H.H. Wong, K.W. Fan, L. Lei, C. Wang, J.C. Baena, H. Okoye, et al., Fire-resistant flexible polyurethane foams via nature-inspired chitosan-expandable graphite Coatings, ACS Appl. Polym. Mater. 3 (8) (2021) 4079–4087.

[23] H. Xie, X. Lai, H. Li, J. Gao, X. Zeng, X. Huang, et al., A highly efficient flame retardant nacre-inspired nanocoating with ultrasensitive fire-warning and self-healing capabilities, Chem. Eng. J. 369 (2019) 8–17.

[24] P. Li, C. Liu, Q. Jiang, Y. Tao, Y. Xu, Y. Liu, et al., Halogen-free coatings combined with the synergistic effect of phytic acid and montmorillonite for fire safety flexible polyurethane foam, Macromol. Mater. Eng. 307 (5) (2022), 2100930.

[25] H. Xie, X. Lai, Y. Wang, H. Li, X. Zeng, A green approach to fabricating nacre-inspired nanocoating for super-efficiently fire-safe polymers via one-step self-assembly, J. Hazard. Mater. 365 (2019) 125–136.

[26] L. Maddalena, F. Carosio, A Fina, *In Situ* assembly of DNA/graphene oxide nanoplates to reduce the fire threat of flexible foams, Adv. Mater. Interfaces 8 (21) (2021), 2101093.

[27] H. Pan, B. Yu, W. Wang, Y. Pan, L. Song, Y. Hu, Comparative study of layer by layer assembled multilayer films based on graphene oxide and reduced graphene oxide on flexible polyurethane foam: flame retardant and smoke suppression properties, RSC Adv. 6 (115) (2016) 114304–114312.

[28] Y.J. Xu, L.Y. Qu, Y. Liu, P. Zhu, An overview of alginates as flame-retardant materials: pyrolysis behaviors, flame retardancy, and applications, Carbohydr. Polym. 260 (2021), 117827.

[29] S. Lazar, B. Eberle, E. Bellevergue, J. Grunlan, Amine salt thickening of intumescent multilayer flame retardant treatment, Ind. Eng. Chem. Res. 59 (7) (2020) 2689–2695.

[30] M.-J. Chen, S. Lazar, T.J. Kolibaba, R. Shen, Y. Quan, Q. Wang, et al., Environmentally benign and self-extinguishing multilayer nanocoating for protection of flammable foam, ACS Appl. Mater. Interfaces 12 (43) (2020) 49130–49137.

[31] F. Cura', R. Sesana, X.-C. Zhang, F. Scarpa, W.J. Lu, H.-X Peng, Stiffness, energy dissipation, and hyperelasticity in hierarchical multilayer composite nanocoated open-cell polyurethane foams, Adv. Eng. Mater. 21 (12) (2019), 1900459.

[32] W. Qi, Z. Xue, W. Yuan, H. Wang, Layer-by-layer assembled graphene oxide composite films for enhanced mechanical properties and fibroblast cell affinity, J. Mater. Chem. B 2 (3) (2014) 325–331.

[33] B. Schartel, T.R. Hull, Development of fire-retarded materials—Interpretation of cone calorimeter data, Fire Mater. 31 (5) (2007) 327–354.

[34] F. Carosio, M. Ghanadpour, J. Alongi, L. Wågberg, Layer-by-layer-assembled chitosan/phosphorylated cellulose nanofibrils as a bio-based and flame protecting nano-exoskeleton on PU foams, Carbohydr. Polym. 202 (2018) 479–487.

[35] C. Bao, Y. Guo, B. Yuan, Y. Hu, L. Song, Functionalized graphene oxide for fire safety applications of polymers: a combination of condensed phase flame retardant strategies, J. Mater. Chem. 22 (43) (2012) 23057–23063.

[36] F. Carosio, L. Medina, J. Kochumalayil, L.A. Berglund, Green and fire resistant nanocellulose/hemicellulose/clay foams, Adv. Mater. Interfaces 8 (18) (2021), 2101111.